Seventh International Conference on Computational Fluid Dynamics (ICCFD7), Big Island, Hawaii, July 9-13, 2012

ICCFD7-2904

Integrated Adaptive Numerical Method for Transient Two-phase Flow in Heterogeneous Porous Media

C.C. Chueh*, W. Bangerth** and N. Djilali*
Corresponding author: ndjilali@uvic.ca

* Inst. for Integrated Energy Systems & Dept. of Mech. Eng., Univ. Victoria, Canada.
** Department of Mathematics, Texas A&M University, College Station, TX, USA.

Abstract: An interconnected set of algorithms is presented for the simulation of two-phase flow in porous media achieving more than two orders of magnitudes acceleration. The methods combine: an adaptive operator splitting technique; adaptive meshing; efficient block preconditioning; and a localized artificial diffusion strategy for stabilization. The accuracy and efficiency of the approach is demonstrated through numerical experiments for three types of flows in heterogeneous porous media, including an advection dominated flow and flow involving capillary transport.

*Keywords:*Adaptive refinement; Stabilized finite element method; Operator splitting; Preconditioning; Two-phase flow; Porous media; Fuel cells.

1 Introduction

Multiphase flow in porous media are ubiquitous in applications ranging from flow of groundwater and secondary oil recovery, to geo-sequestration of carbon dioxide and transport processes in fuel cell electrodes [1]. The simulation of such flows poses a number of physical and computational modelling challenges. In the case of polymer electrolyte membrane fuel cells (PEMFCs) which motivated this work, porous media play a crucial role in the transport of reactants (hydrogen and oxygen) and of the products of the electrochemical energy conversion process, *viz.* electric current, water and heat. The transport is facilitated in the so-called membrane-electrode-assembly via two key porous media: the gas diffusion layer (GDL) and the catalyst layer. When the fuel cell operates at higher currents, or when local water and/or heat management are inadequate, water condensation can lead to "flooding" within the porous GDL and catalyst layer. The resulting blockage of pores hinders the diffusion of reactant gases, and can lead to local starvation of the reaction sites and, in turn, severe performance losses and potential degradation. The understanding and prediction of the two-phase transport in GDLs and other components of a fuel cell is a pacing item in the development of fuel cell technology, as it affects not only performance, but also durability. The GDL is a heterogeneous anisotropic porous medium consisting of fibres that are treated to impart hydrophobicity in order to promote water removal. The complexity of the medium, the lack of fundamental understanding regarding effective transport properties and constitutive relations, the couplings and the transient nature of the flows make simulation of multiphase flow in porous media difficult.

The background and salient issues related to the numerical solution of flow in porous media are reviewed in [2]. Effective stabilization of higher order methods is an important ingredient for achieving computational efficiency without compromising accuracy. We have previously shown that an extension of the entropy-based artificial viscosity approach proposed by Guermond & Pasquetti [3] does ensure stability and accuracy when used in conjunction with a general continuous finite element discretization for two phase flow in porous media [4] provided the term acts only in the vicinity of strong gradients in the saturation and other discontinuities. Although adaptive methods have been the subject of many developments, see, e.g. [5, 6], with the h-adaptive methods being the most commonly used in engineering applications, the literature on adaptive techniques for *transient* multiphase flow in porous media is relatively scarce. The coupling between the flow and pressure

field and individual phase transport is usually dealt with using classical operator splitting techniques (e.g. [7]). While this effectively decouples the flow and saturation transport equations, significant computing resources are still required to solve the velocity-pressure equation at each time step, making simulations costly.

In this this work we focus on the key issues of enhancing computational efficiency of finite element methods while retaining accuracy, and we present and apply a computational framework integrating the following features: (i) higher order spatial discretization yielding the same accuracy at smaller computational cost, and incorporating stabilization mechanisms for hyperbolic problems such as those representing multiphase flow; (ii) adaptive mesh refinement that vastly reduces the number of cells required to resolve the flow field; (iii) adaptive operator splitting and time stepping that allows the use of large time step limited solely by the physical time scale rather than numerical stability; (iv) an operator splitting algorithm allowing the use of efficient solvers; (v) an efficient solver and preconditioning method that accelerate the solution of the linear problem.

These methods were implemented and integrated using the `deal.II` open source finite element library [8], and their application is illustrated in this paper for several heterogeneous porous media problems involving two immiscible phases.

2 Problem Statement

2.1 Governing Equations

We consider incompressible isothermal flow of two immiscible phases. Using the mixture model [9] the macroscopic equations governing the flow in a 16ilic porous media characterized by a porosity ϵ and a permeability tensor $\mathbf{K}$ can be expressed as [10]

$$\mathbf{u}_t = -\lambda_t \mathbf{K} \nabla p_w - \lambda_{nw} \mathbf{K} \nabla p_c \tag{1}$$

$$\nabla \cdot \mathbf{u}_t = q_w + q_{nw} \tag{2}$$

$$\epsilon \frac{\partial S_w}{\partial t} + \nabla \cdot (F \mathbf{u}_t) + \nabla \cdot (\lambda_{nw} F \mathbf{K} \nabla p_c) = q_w \tag{3}$$

where the total velocity $\mathbf{u}_t = \mathbf{u}_w + \mathbf{u}_{nw}$; S is the saturation (volume fraction) with subscripts w and nw denoting the wetting and non-wetting phase respectively with $S_w + S_{nw} = 1$; q is a source term. The capillary pressure is given by

$$p_c = p_{nw} - p_w \tag{4}$$

and the total mobility λ_t and the fractional flow of the wetting phase F are defined by

$$\lambda_t = \lambda_w + \lambda_{nw} = \frac{k_{rw}}{\mu_w} + \frac{k_{rnw}}{\mu_{nw}} \tag{5}$$

$$F(S) = \frac{\lambda_w}{\lambda_t} = \frac{\lambda_w}{\lambda_w + \lambda_{nw}} = \frac{k_{rw}/\mu_w}{k_{rw}/\mu_w + k_{rnw}/\mu_{nw}} \tag{6}$$

where k_r is the relative permeability and μ the viscosity.

In order to close the set of governing equations it is also necessary to prescribe a constitutive relation for the capillary pressure, discussed further below, as well as the relative permeability. Following a commonly used prescription for the dependence of the relative permeabilities k_{rw} and k_{rnw} on saturation, we use

$$k_{rw} = S_e^n, \qquad k_{rnw} = (1 - S_e)^n . \tag{7}$$

The effective saturation S_e is defined in the next subsection. The exponent n depends on the capillary parameter characterizing the porous medium; capillary pore network simulations [11] yield $1.7 < n < 2.8$. A value of $n = 2$ is used for the simulation with negligible capillary transport, and a value of 3 for simulation accounting for capillary transport.

It should be noted that the form of equations (1) and (3) corresponds to the case of a *hydrophylic* medium. For the the hydophobic case, it is more convenient to solve the equations in terms of the non-wetting phase

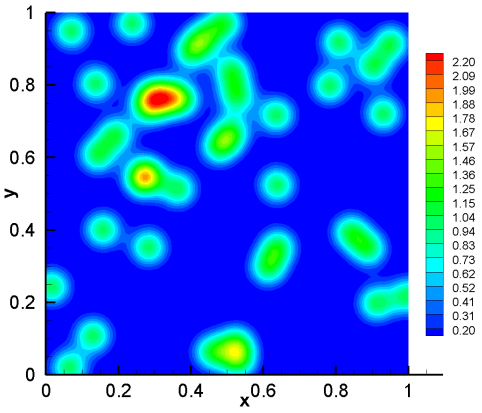

Figure 1: Illustration of random permeability field.

and these equations can be recast accordingly [10]. For flow situations where capillary transport is negligible, the capillary pressure is simply set to zero.

With the required parameters and constitutive relations prescribed, equations (1)–(3) can be solved subject to appropriate initial conditions for saturation and boundary conditions for pressure.

2.2 Capillary Pressure Function

The capillary pressure p_c is correlated as a function of both S_w and k both based on the so-called Leverett J-function [12, 13]:

$$J\left(S_e\right) = \frac{p_c}{\sigma_c \cos\left(\theta_c\right)} \left(\frac{k}{\epsilon}\right)^{1/2} \tag{8}$$

where σ_c is the surface tension, k is the permeability and θ_c is the contact angle, which varies between 0° and 90° for hydrophilic media.

The effective saturation S_e is defined in terms of the so-called immobile or irreducible saturation [14, 15, 9], which represents a threshold value below which liquid remains immobile (no capillary transport),

$$S_e = \begin{cases} \frac{S_w - S_{irr}}{1 - S_{irr}} & \text{for} \quad 0^\circ < \theta_c \leq 90^\circ \\ \\ \frac{S_{nw} - S_{irr}}{1 - S_{irr}} & \text{for} \quad 90^\circ < \theta_c \leq 180^\circ \end{cases} \tag{9}$$

The pressure-saturation relationship (J-function) is prescribed following the classic correlation of Udell[16] for hydrophilic media:

$$J\left(S_e\right) = 1.417\left(1 - S_e\right) - 2.120\left(1 - S_e\right)^2 + 1.263\left(1 - S_e\right)^3$$

Further details on how the J-function is incorporated in the governing equation, and the final form of the solved equations is given in [10].

2.3 Physical System and Boundary Conditions

The application of the integrated methods to 2D and 3D problems involving two-phase flow without capillary transport in heterogeneous media is discussed in [4, 2]. Here we consider primarily capillary transport in a

hydrophilic medium characterized by a pseudo-random permeability given by

$$k_{rm}(\mathbf{x}) = \min\left\{\max\left\{\sum_{l=1}^{N_p}\Psi_l(\mathbf{x}), 0.01\right\}, 4\right\} \tag{10}$$

$$\Psi_l(\mathbf{x}) = \exp\left(-\left(\frac{|\mathbf{x}-\mathbf{x}_l|}{B_w}\right)^2\right)$$

where the centres $\mathbf{x}_l$ are N_p random locations of higher permeability inside the domain and B_w is the band width of the exponential function. The permeability function is bounded both above and below to limit the size of the condition number of the discretized problem [17]. Figure 1 shows the permeability field contour with $N_p = 40$.

The simulations are performed on a computational domain $\Omega = [0,1] \times [0,1]$ in 2D and $\Omega = [0,1] \times [0,1] \times [0,1]$ in 3D for $t \in [0,T]$. The initial condition is set to $S_w(\mathbf{x},0) = 0$. The boundary conditions for the velocity/pressure equations are prescribed on all the boundaries as follows:

$$p_w(\mathbf{x},t) = 0 \qquad \text{on} \quad \partial\Omega$$

Boundary conditions for the saturation transport equation are only imposed on inflow boundaries.

$$S_w(\mathbf{x},t) = 0 \qquad \text{on} \quad \mathbf{\Gamma}_{in}(t) = \{\mathbf{x} \in \partial\Omega : \mathbf{n}\cdot\mathbf{u}_t < 0\}$$

3 Numerical method

It was noted in the Introduction that the numerical solution of the system of partial differential equations governing two-phase transport is computationally costly. The simulations presented here were performed using a framework integrating several methods to address the key issue to ensure computational efficiency: stabilized higher order spatial discretization; adaptive mesh refinement; adaptive time stepping; efficient solver and preconditioning. The methods were implemented using the deal.II open source finite element library [8, 18]. The details of the implementation, validation and numerical experiments in porous media flows without capillary transport are reported in [2], demonstrating the accuracy of the approach and a two-order of magnitude speedup. In this paper the methodology is extended to account for capillary transport as described in Section 2.3. The features of the computational framework are summarized below.

Adaptive operator splitting and time stepping: The time stepping schemes most commonly used to solve the type of equations (1) and (3) are of IMPES (*implicit pressure, explicit saturation*) type. Noting that the pressure and velocity fields depend only weakly on saturation, a net reduction in computing time can be achieved by rebalancing the computing efforts between the saturation and the pressure/velocity system. An operator splitting approach was implemented to achieve this by solving for the saturation at every time step, and only updating the velocity and pressure whenever necessary at specific "macro time-steps". A key feature is letting the length of the macro time-steps vary *adaptively* as a function of the saturation rate of changes.

Spatial discretization and adaptive mesh refinement: The IMPES scheme requires the separate solution of velocity/pressure and saturation equations. Using a finite element method, we discretize these on the same mesh composed of quadrilaterals or hexahedra, using continuous Q_2 elements for the velocity and Q_1 elements for the pressure. Continuous Q_1 finite elements are also used to discretize the saturation equation. This choice is primarily predicated by the capillary pressure (diffusion) term, as the discretization of the Laplace operator using the more popular discontinuous Galerkin (DG) methods leads to a significant number of additional terms that need to be integrated and have the drawback of artificial diffusion acting everywhere. A shock-type adaptive refinement method described in [4] is used.

Artificial diffusion stabilization of the saturation equation: The Q_1 elements for the saturation equation require stabilization. To avoid smearing of sharp fronts and grid-orientation difficulties associated with classical artificial diffusion, we use the artificial diffusion term proposed by Guermond and Pasquetti [3],

which acts primarily in the vicinity of discontinuities and therefore allows a higher degree of accuracy. An explicit Euler time stepping method is used to avoid the difficulty of dealing with the non-linear stabilization term.

Solver and preconditioning: The linear systems to be solved are typically ill-conditioned, non-symmetric and/or indefinite, with a size that essentially restricts the choice to Krylov subspace methods. Good preconditioning is hence essential for computational efficiency. In porous media flows, an additional complication is the saddle point structure of the problem. There is a vast literature on preconditioning techniques for such problems; a method originally proposed for the Stokes system by Silvester and Wathen [19] leads to very efficient and adjustable preconditioners and is adapted to the set of equations solved here.

4 Results and Discussion

Prior to presenting sample simulations involving capillary transport, we first verify and assess the method using the classical Buckley-Leverett benchmark problem which exhibits a shock well suited to test the adaptivity and accuracy of the method.

4.1 Numerical Validation: Advection Dominated Flow

The Buckley-Leverett problem describes transient displacement in a *homogeneous* medium without capillary effects. The problem is set up by $p_c = 0$ and prescribing the following boundary conditions:

$$\begin{aligned} p(\mathbf{x},t) &= 1 - x \qquad \text{on} \quad \partial\Omega \times [0,T]. \\ S(\mathbf{x},t) &= 1 \qquad \text{on} \quad \mathbf{\Gamma}_{in}(t) \cap \{x = 0\} \\ S(\mathbf{x},t) &= 0 \qquad \text{on} \quad \mathbf{\Gamma}_{in}(t) \backslash \{x = 0\} \end{aligned}$$

This corresponds to invasion of the domain by the wetting phase from the left boundary. Note that pressure and saturation uniquely determine a velocity, and the velocity determines whether a boundary segment is an inflow or outflow boundary. No outflow boundary conditions are required for the saturation.

The parameters used in the simulation are given in Table 1. The results in Figure 2 are compared to previous simulations using discontinuous Galerkin space [17]. The saturation profiles obtained with the two methods are essentially identical, but significantly fewer degrees of freedom are required in the adaptive mesh solution, which was obtained also with adaptive operator splitting. The shock capturing capability and the effectiveness of the localized diffusive stabilization method are clearly illustrated; for an in-depth verification of the efficiency and accuracy, see [4, 2].

Table 1: Parameters used in the Buckley-Leverett problem

PARAMETER	SYMBOL	VALUE	UNIT
Porosity	ϵ	1.0	-
Viscosity (wetting)	μ_w	0.2	$g \cdot cm^{-1} \cdot sec^{-1}$
Viscosity (nonwetting)	μ_{nw}	1.0	$g \cdot cm^{-1} \cdot sec^{-1}$
permeability (constant)	k	0.1	cm^2

4.2 Hydrophilic Porous Medium

We consider here capillary dominated transport in a medium having a single source $q_w = 2$ (sec^{-1}) located at the center of the domain. The immobile saturation S_{irr} is set to zero, and the surface tension σ_c to 10^{-2} $g \cdot sec^{-2}$. The evolution of the saturation field and the corresponding mesh are shown in Figure 3. The transport is driven by the combination of pressure gradient and capillary (diffusive) effects associated with both saturation and permeability gradients which both act by transporting the wetting-phase from high to low values of S_w and k. One notable aspect of the effect of permeability gradients in this heterogeneous

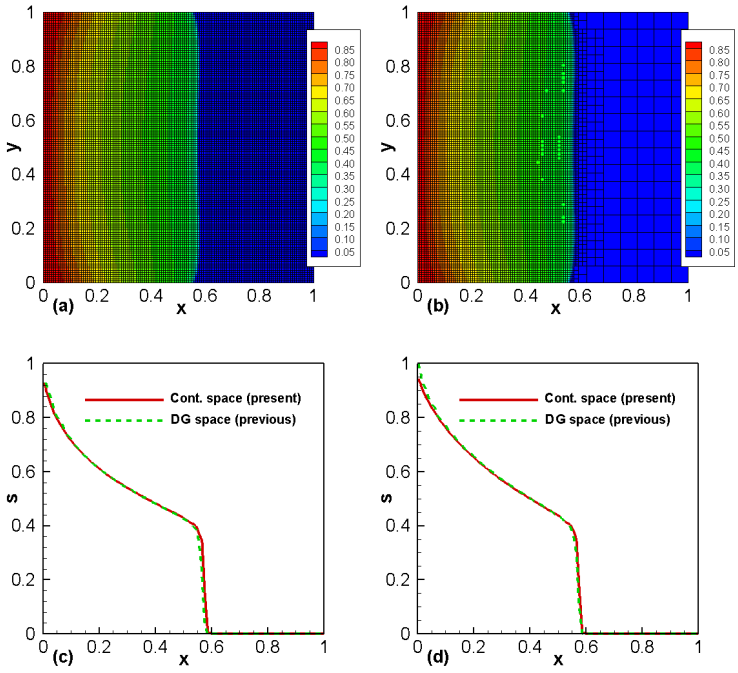

Figure 2: 2D Benchmark simulation of invasion in a uniform porous medium: comparison with previous work of Li and Bangerth [17] at $t = 2.78$: (a) Saturation field using discontinuous Galerkin space[17]. (b) Saturation field using continuous space with the stabilizing term and operator splitting (present work). (c) Saturation profile along $y = 0.5$. (d) Saturation profile along $y = 0.9$.

medium is the isolation of the wetting-phase. The saturation contours show that the wetting-phase, which is surrounded by three high-permeability areas on the top, left and right sides of $(0.5, 0.5)$, diffuses initially through a throat-like path around $(0.45, 0.55)$ and then reaches a triangle-shaped area around $(0.39, 0.65)$ surrounded by few high-permeability regions. The wetting-phase fluid subsequently accumulates inside this triangular area. In fact, during the process, the wetting-phase doesn't flow through high-permeability regions but rather through low-permeability areas (cf. Figure 1), which is counter-intuitive. This phenomenon is due to the saturation gradients that drive the fluid in three directions (i.e. top, left and right directions) while permeability gradient act in the opposite directions. The combined effect of these mechanisms together with pressure is a transport pattern taking place primarily through lower permeability regions.

Both grid refinement and coarsening are clearly shown in Figure 3. The total number of degrees of freedom for the adaptive method increases with time as the wetting-phase gradually spreads in the porous medium, but in any case there is a significant reduction in the required mesh compared to the (static) uniform mesh simulation as shown in Figure 4. Overall, the required number of DoFs is reduced by over 90% at the beginning of the simulation cycle and by over 40% at the end. As a result, there is a twofold net reduction in computational time over the cycle due solely to adaptive mesh refinement.

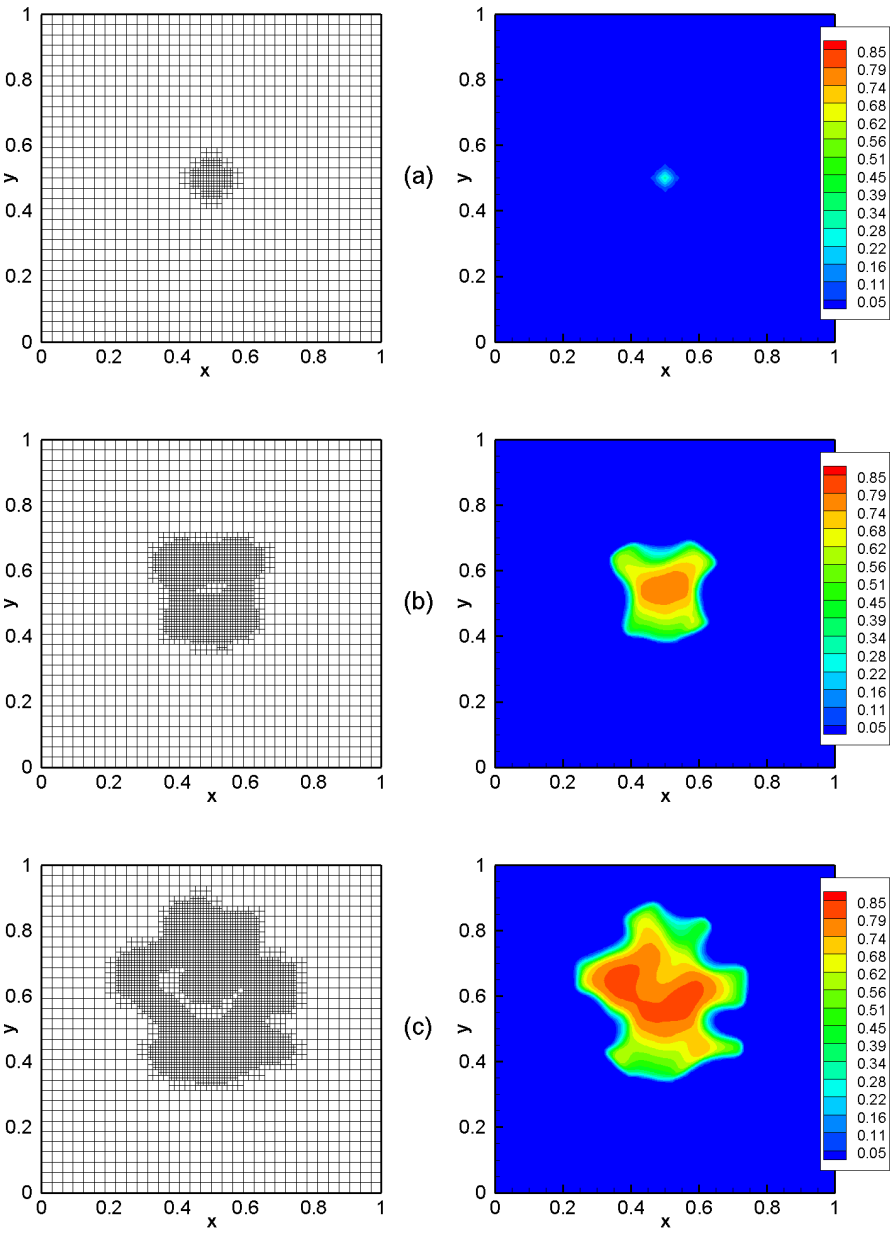

Figure 3: Hydrophilic medium: time evolution of wetting-phase saturation contours (right) and corresponding grids. (a) $t = 0.016$ *sec*; (b) $t = 3.079$ *sec*; (c) $t = 5.882$ *sec*.

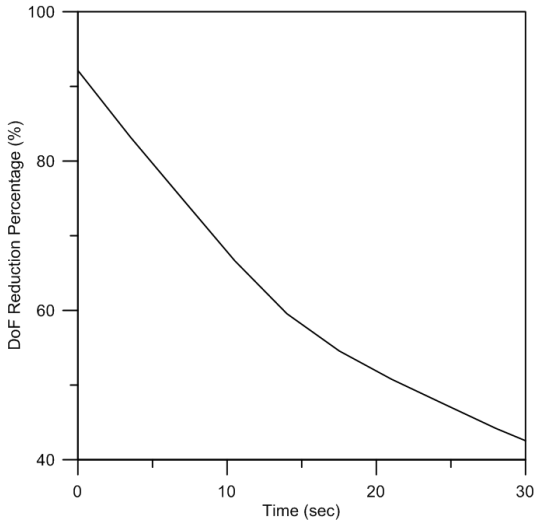

Figure 4: Reduction of required DoF relative to uniform grid.

5 Conclusion and Future Work

To address the needs for high resolution methods with improved computational efficiency to simulate two-phase flow in porous media, we have presented an integrated set of methods incorporating (i) an adaptive operator splitting method that only recomputes the velocity and pressure variables whenever necessary; (ii) block matrix preconditioning methods that greatly reduce the computing time; (iii) an entropy-based stabilizing term that preserves accuracy and ensures stability; and (iv) locally adaptive refinement allowing highly resolved time dependent simulations. The robustness and effectiveness of this computational framework was demonstrated in two types of porous media flows one of which includes flow with capillary transport.

The techniques described in this paper are sufficiently general to apply to a wide range of two-phase flow porous flow problems. The techniques have been implemented in an open source framework [20] that should allow further developments to account for additional complexities such as multiple interacting phases. Furthermore the underlying numerical methods are well suited for parallelization, which would further enhance computational efficiency.

References

[1] N Djilali and PC Sui. Transport phenomena in fuel cells: from microscale to macroscale. *International Journal of Computational Fluid Dynamics*, 22(1-2):115–133, 2008.

[2] CC Chueh, N Djilali, and W Bangerth. An h-adaptive operator splitting method for two-phase flow in 3d heterogeneous porous media. *under review, SIAM J. Scientific Computing.*

[3] JL Guermond and R Pasquetti. Entropy-based nonlinear viscosity for fourier approximations of conservation laws. *Comptes Rendus Mathematique*, 346(13-14):801–806, 2008.

[4] CC Chueh, M Secanell, W Bangerth, and N Djilali. Multi-level adaptive simulation of transient two-phase flow in heterogeneous porous media. *Computers and Fluids*, 39:1585–1596, 2010.

[5] R Hinkelmann. *Efficient Numerical Methods and Information-Processing Techniques in Environment Water*. Habilitation, Universität Stuttgart, 2002.

[6] W Bangerth and R Rannacher. *Adaptive Finite Element Methods for Differential Equations*. Birkhäuser Verlag, 2003.

[7] KH Karlsen, KA Lie, JR Natvig, HF Nordhaug, and HK Dahle. Operator splitting methods for systems of convection-diffusion equations: Nonlinear error mechanisms and correction strategies. *Journal of Computational Physics*, 173(2):636–663, 2001.

[8] W Bangerth, R Hartmann, and G Kanschat. deal.II – a general purpose object oriented finite element library. *ACM Trans. Math. Softw.*, 33(4):24/1–24/27, 2007.

[9] S Litster and N Djilali. *Two-phase transport in porous gas diffusion electrodes (Eds. M. Faghri & B. Sunden)*. WIT Press, Southampton, UK, 2005.

[10] CC Chueh. *Adaptive computational analysis of transient two-phase mixture flow in heterogeneous porous media with application to diffusion media of proton exchange membrane fuel cells*. PhD Dissertation, University of Victoria, Canada http://www.iesvic.uvic.ca/publications/doctoral_dissertations.php, 2010.

[11] B Markicevic, A Bazylak, and N Djilali. Determination of transport parameters for multiphase flow in porous gas diffusion electrodes using a capillary network model. *Journal of Power Sources*, 171(2):706–717, 2007.

[12] MC Leverett. Capillary behaviour in porous solids. *AIME Trans.*, 142:152–169, 1941.

[13] JH Nam and M Kaviany. Effective diffusivity and water-saturation distribution in single-and-two layer PEMFC diffusion medium. *International Journal of Heat and Mass Transfer*, 46:4595–4611, 2003.

[14] J Bear. *Dynamics of Fluids in Porous Media*. American Elsevier, 1972.

[15] M Kaviany. *Principles of Heat Transfer in Porous Media*. Springer-Verlag, New York, 1991.

[16] KS Udell. Heat transfer in porous media considering phase change and capillary - the heat pipe effect. *International Journal of Heat and Mass Transfer*, 28(2):485–495, 1985.

[17] Y Li and W Bangerth. *The deal.II tutorial manual: step-21*. http://dealii.org/developer/doxygen/deal.II/step_21.html.

[18] W Bangerth, R Hartmann, and G Kanschat. `deal.II` *Differential Equations Analysis Library, Technical Reference*, 2010. `http://www.dealii.org/`.

[19] D Silvester and A Wathen. Fast iterative solution of stabilised stokes systems part ii: Using general block preconditioners. *SIAM Journal on Numerical Analysis*, 31(5):1352–1367, 1994.

[20] CC Chueh and W Bangerth. *The deal.II tutorial manual: step-43*. http://dealii.org/developer/doxygen/deal.II/step_43.html.